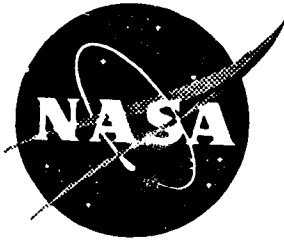This microfiche was produced according to ANSI / AIIM Standards and meets the quality specifications contained therein. A poor blowback image is the result of the characteristics of the original document.

A Non-local Computational Boundary Condition for Duct Acoustics

William E. Zorumski and Willie R. Watson
Langley Research Center, Hampton, Virginia

Steve L. Hodge
Virginia Consortium of Engineering and Science Universities, Hampton, Virginia

March 1994

Abstract

A non-local boundary condition is formulated for acoustic waves in ducts without flow. The ducts are two-dimensional with constant area, but with variable impedance wall lining. Extension of the formulation to three-dimensional and variable area ducts is straightforward in principle, but requires significantly more computation. The boundary condition simulates a non-reflecting wave field in an infi. ite duct. It is implemented by a constant matrix operator which is applied at the boundary of the computational domain. An efficient computational solution scheme is developed which allows calculations for high frequencies and long duct lengths. This computational solution utilizes the boundary condition to limit the computational space while preserving the radiation boundary condition. The boundary condition is tested for several sources. It is demonstrated that the boundary condition can be applied close to the sound sources, rendering the computational domain small. Computational solutions with the new non-local boundary condition are shown to be consistent with the known solutions for nonreflecting wavefields in an infinite uniform duct.

i

1 Introduction

The emerging field of computational aeroacoustics addresses the resolution of short wavelength and small amplitude motions of compressible fluids [1]. These problems are typically posed on unbounded domains, which present special problems for numerical techniques which use grids as there are a finite number of grid points to fit in an infinite domain. Typically the grid points are spaced far apart in the farfield, meaning significant loss of the accuracy necessary for computational aeroacoustics.

To limit the number of gridpoints, the domain is separated into a bounded part, which is gridded, and an unbounded part, which is treated analytically. The approach of this paper is to assume that the unbounded, or exterior, domain is governed by a wave equation with a known general solution in terms of an eigenfunction expansion. To couple the bounded, or interior, domain and the exterior domain, it is not necessary to completely specify the exterior solution at the interface. Rather, at the interface, a relationship between the modal components of the exterior solution variables is expressed via a *matrix impedance operator*. The end result is that a computational solution is performed in the interior domain with the exterior solution replaced completely by a special boundary condition at the interior/exterior interface. In current parlance, the boundary condition is referred to as "nonlocal", in contrast to the classical "local" Neuman or Dirichlet boundary conditions, or the well known approximations of pseudodifferential operators [2].

It is assumed here that efficient and accurate solutions to problems in computational aeroacoustics depend as much on the computational boundary conditions as they depend on the interior algorithms. If accurate boundary conditions are specified at the surface of a small interior, the computational domain then is usually small and the physical phenomena may be accurately captured with computational economy. This assumption is examined using several sources in an infinite duct. These problems have classical analytic solutions in terms of an infinite series of duct modes.

The boundary operator, the *nodal impedance* operator is shown to be a similarity trans-

1

formation of a diagonal matrix operator whose elements are the *modal impedances* of individual waves in the classical solution to the exterior operator. The transformation matrix is constructed by evaluating each *mode* in the exterior solution at each *node* in the interior solution.

Section 2 of this paper defines basic equations used in the computation and formally states the non-local boundary condition. The derivation of the similarity transformation for the boundary operator is given in section 3. Results and discussion of several source solutions and frequencies are given in section 4. Appendix A describes the numerical method, a finite element procedure, and Appendix B gives the details of the infinite-duct eigenvalue computations. These eigenvalue computations are a crucial step, since the computation of the boundary operator requires the same number of eigenvalues as boundary node points. This may be a large number for the high-frequency cases, so that provision must be made for evaluating an essentially unlimited number of eigenvalues. Conclusions, relative to the basic assumptions of the paper, are given in section 5.
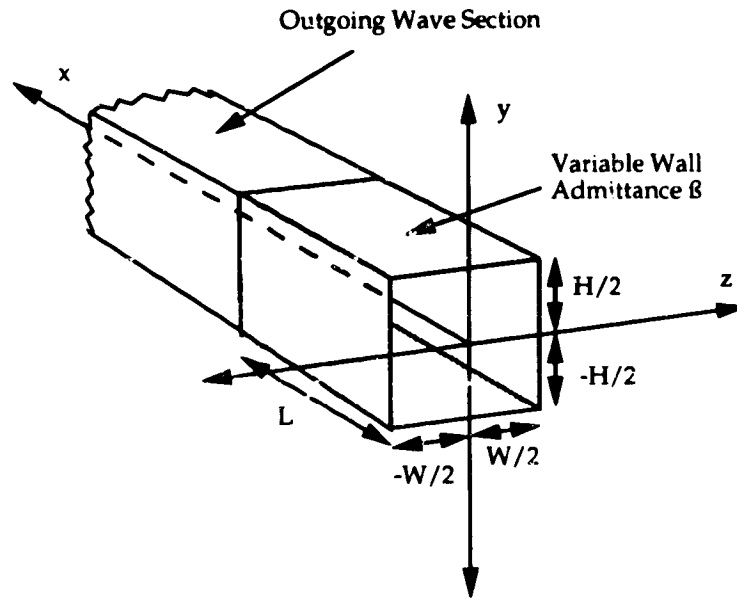
Figure 1: Infinitely long three dimensional duct and coordinate system.

2 Computational Solution

Consider a three-dimensional rectangular duct filled with a homentropic fluid within the region $\frac{-H}{2} \leq y \leq \frac{H}{2}$ and $\frac{-W}{2} \leq z \leq \frac{W}{2}$ as shown in figure 1. Acoustic waves in a duct are governed by the linearized equations of mass, momentum and energy [3]. The background pressure $(\bar{p})$ and background density $(\bar{\rho})$[1] are assumed constant and the background flow velocity components are zero. Under these assumptions the sound speed $\bar{c}$ is related to the steady density and pressure by the equation

$$\bar{c}^2 = \frac{\gamma \bar{p}}{\bar{\rho}} \tag{1}$$

The duct is assumed infinitely long in the axial direction with a known velocity source at the plane $x = 0$. The walls of the duct contain sound absorbing material whose material properties vary arbitrarily both around the circumference and along the axis of the duct for $0 \leq x \leq L$. Within the region $L \leq x \leq \infty$ the material properties of the liner are assumed uniform, so that the wave field generated by the source will be that of an outgoing wave in

---

[1] or equivalently "mean" or "ambient" pressure or density (see [3])

3

this region. "Steady state" acoustic wave solutions are defined to be solutions of the form

$$\begin{Bmatrix} \tilde{\rho} \\ \tilde{u} \\ \tilde{v} \\ \tilde{w} \\ \tilde{p} \end{Bmatrix} = \begin{Bmatrix} \hat{\rho} \\ \hat{u} \\ \hat{v} \\ \hat{w} \\ \hat{p} \end{Bmatrix} e^{i\omega t} \tag{2}$$

in which $\hat{\rho}, \hat{u}, \hat{v}, \hat{w},$ and $\hat{p}$ respectively denote the acoustic density, axial component of acoustic velocity, transverse component of acoustic velocity, spanwise component of acoustic velocity and acoustic pressure in the duct.

Using (2), the acoustic equations are now a set of time independent equations given by

$$\begin{bmatrix} i\omega & \bar{\rho}\frac{\partial}{\partial x} & \bar{\rho}\frac{\partial}{\partial y} & \bar{\rho}\frac{\partial}{\partial z} & 0 \\ 0 & i\omega & 0 & 0 & \frac{1}{\bar{\rho}}\frac{\partial}{\partial x} \\ 0 & 0 & i\omega & 0 & \frac{1}{\bar{\rho}}\frac{\partial}{\partial y} \\ 0 & 0 & 0 & i\omega & \frac{1}{\bar{\rho}}\frac{\partial}{\partial z} \\ 0 & \gamma\bar{p}\frac{\partial}{\partial x} & \gamma\bar{p}\frac{\partial}{\partial y} & \gamma\bar{p}\frac{\partial}{\partial z} & i\omega \end{bmatrix} \begin{Bmatrix} \hat{\rho} \\ \hat{u} \\ \hat{v} \\ \hat{w} \\ \hat{p} \end{Bmatrix} = \{0\} \tag{3}$$

It is assumed that the wall boundary conditions are expressed through the *acoustic admittances* β of the sound absorbing material. These parameters relate the velocity normal to the wall to the pressure at the wall; that is,

$$-\hat{v} = \beta\hat{p}, \quad y = -\frac{H}{2} \tag{4}$$

$$+\hat{v} = \beta\hat{p}, \quad y = +\frac{H}{2} \tag{5}$$

$$-\hat{w} = \beta\hat{p}, \quad z = -\frac{W}{2} \tag{6}$$

$$+\hat{w} = \beta\hat{p}, \quad z = +\frac{W}{2} \tag{7}$$

Equations (3) along with equations (4)–(7) are respectively the differential equations and wall boundary conditions governing linear acoustic disturbances of frequency ω in the duct. When coupled to the source and a radiation condition, they can in theory be solved uniquely to obtain the attenuation over a specified length of lining.

The interior duct calculation is terminated at $x = L$ and a *nonreflecting nonlocal* boundary condition, described below, is applied to close off the numerical calculation. The calculations are limited to two-dimensions for reasons of economy. Extension to three-dimensions is

4

straightforward, but requires significantly more computation. The two dimensional analysis to follow is obtained by assuming planar waves across the duct, so that the wave field in independent of z (terms with $\frac{\partial}{\partial z}$ fall out of (3)).

The elements of the two-dimensional counterpart of equation (3) are combined into a second order differential equation containing the acoustic pressure [3]:

$$\nabla^2 \hat{p} + k^2 \hat{p} = S \tag{8}$$

where

$$k = \frac{\omega}{\bar{c}} \tag{9}$$

is the freespace wavenumber and ∇^2 is the Laplace operator in the (x, y) plane. A source S has been introduced in order to generate non-trivial solutions. The wall boundary condition may be expressed in terms of the acoustic pressure only:

$$\vec{\nabla}\hat{p} \cdot \vec{n} + ik\bar{\rho}\bar{c}\beta\hat{p} = 0 \tag{10}$$

in which $\vec{\nabla}$ is the vector gradient, vector $\vec{n}$ the unit normal vector to the liner surface and "·" is the vector dot product.

There remains the duct termination condition at $x = L$. Because the portion of duct for $x \geq L$ is considered infinite and uniform, the wave field in this section of duct is expected to propagate out to infinity without reflecting. The boundary condition at $x = L$ achieves this objective. The condition itself is a linear relationship between the acoustic pressure and the normal component of acoustic velocity at $x = L$ of the form

$$\{\hat{p}_i\} = [Z_{ij}]\{\hat{u}_j\} \tag{11}$$

$$[Z_{ij}] = \begin{bmatrix} Z_{11} & Z_{12} & \cdots & Z_{1M} \\ Z_{21} & Z_{22} & \cdots & Z_{2M} \\ \vdots & \vdots & \ddots & \vdots \\ Z_{M1} & Z_{M2} & \cdots & Z_{MM} \end{bmatrix}. \tag{12}$$

Here $\{\hat{p}_i\}$ and $\{\hat{u}_j\}$ are $M \times 1$ column matrices containing the acoustic pressure and the normal component of acoustic velocity, respectively, along the boundary nodes at $x = L$. A

method for determining the complex coefficients in the $M \times M$ matrix $[Z_{ij}]$ is given in the following section for the case of an infinite duct. The general form, however, is valid for any duct, and may include, for example, the effects of radiation conditions at the end of a finite duct [4].

Equations (8) and (10) are solved numerically using a finite element method. Details of the numerical implementation are given in appendix A. The results are used to evaluate the performance of the wall lining over the length L. The following expression is used to evaluate the acoustic intensity at a point (x,y) in the duct [7]:

$$I(x,y) = \frac{1}{2}\Re\left[\hat{p}\hat{u}^*\right] = \frac{-1}{2\omega\bar{\rho}}\Re\left[i\hat{p}\frac{\partial\hat{p}^*}{\partial x}\right] \tag{13}$$

where the superscript asterisk denotes the complex conjugate and $\Re$ is the real part.. The attenuation of the lining in decibels is then obtained from

$$\Delta dB = 10\log_{10}\frac{W(0)}{W(L)} \tag{14}$$

where

$$W(x) = \int_{-\frac{H}{2}}^{\frac{H}{2}} I(x,y)dy. \tag{15}$$

is the axial power. To obtain $W(x)$, the integration in equation (15) was performed numerically from the computational solution. The accuracy of the boundary condition is assessed by comparing the numerically computed sound power to computed values of the sound power determined from truncated exact analytic series solutions of the reduced wave equation describing outgoing waves in an infinite duct.

3   Infinite Duct Radiation Condition

Modal solutions to the homogeneous form of equation (8) are

$$p_m^{\pm}(x,y) = \phi_m(y)e^{\mp ik_{xm}(x-L)} \tag{16}$$

where $\phi(y)$ is the mode function

$$\phi_m(y) = Ae^{-ik_y y} + Be^{+ik_y y} \tag{17}$$

The admittance boundary conditions *define* the eigenvalues k_y and eigenvector $\lfloor a \quad b \rfloor^T$ as solutions of a homogeneous matrix equation for the vector $\lfloor a \quad b \rfloor^T$. If the upper wall admittance is $\beta(H/2) = \beta_u$ and the lower wall admittance is $\beta(-H/2) = \beta_l$, then from (3) along with boundary conditions (4)-(7) and (9) it follows that

$$\begin{bmatrix} (k_y - k\bar{\rho}\bar{c}\beta_u)e^{-ik_y H/2} & -(k_y + k\bar{\rho}\bar{c}\beta_u)e^{+ik_y H/2} \\ -(k_y + k\bar{\rho}\bar{c}\beta_l)e^{+ik_y H/2} & (k_y - k\bar{\rho}\bar{c}\beta_l)e^{-ik_y H/2} \end{bmatrix} \begin{Bmatrix} a \\ b \end{Bmatrix} = \begin{Bmatrix} 0 \\ 0 \end{Bmatrix} \tag{18}$$

The determinant of the above matrix must be zero, which is the eigenvalue equation

$$1 = e^{-2ik_y H} \left(\frac{k_y - k\bar{\rho}\bar{c}\beta_u}{k_y + k\bar{\rho}\bar{c}\beta_u} \right) \left(\frac{k_y - k\bar{\rho}\bar{c}\beta_l}{k_y + k\bar{\rho}\bar{c}\beta_l} \right) \tag{19}$$

A method of solving this transcendental equation for values k_y is given in appendix B. The solution for the eigenvalues is a crucial step in the method. Fortunately, the solution method given in appendix B can easily generate thousands of eigenvalues (solutions of (19)) so that eigenvalue generation is not a problem.

Assuming a discrete set of eigenvalues k_{ym}, the corresponding modal functions $\phi_m(y)$ are orthogonal. The eigenvector $\lfloor a \quad b \rfloor^T$ is normalized such that the inner product of two modes is a Kronecker delta function

$$\int_{-H/2}^{+H/2} \phi_m(y)\phi_n(y) = \delta_{mn} \tag{20}$$

The pressure in a field of progressive waves in an infinite duct is

$$\dot{p}(x,y) = \sum_{m=0}^{\infty} \dot{p}_m^+ \phi_m(y)e^{-ik_{xm}(x-L)} \tag{21}$$

7

The corresponding axial velocity amplitude is

$$\hat{u}(x,y) = \sum_{m=0}^{\infty} \hat{u}_m^+ \phi_m(y) e^{-\imath k_{xm}(x-L)} = \frac{1}{\bar{\rho}\bar{c}} \sum_{m=0}^{\infty} \left(\frac{k_{xm}}{k}\right) \hat{p}_m^+ \phi_m(y) e^{-\imath k_{xm}(x-L)} \qquad (22)$$

If we define the modal impedance as

$$\mathcal{Z}_m = \bar{\rho}\bar{c}\frac{k}{k_{xm}} \qquad (23)$$

and relate modal pressure and velocity amplitudes by

$$\hat{p}_m^+ = \mathcal{Z}_m \hat{u}_m^+ \qquad (24)$$

then the pressure and velocity fields can be given in more compact forms as

$$\hat{p}(x,y) = \sum_{m=0}^{\infty} \mathcal{Z}_m \hat{u}_m^+ \phi_m(y) e^{-\imath k_{xm}(x-L)} \qquad (25)$$

$$\hat{u}(x,y) = \sum_{m=0}^{\infty} \hat{u}_m^+ \phi_m(y) e^{-\imath k_{xm}(x-L)} \qquad (26)$$

Matrix expressions, assuming a finite number of modes M, for the pressure and axial velocity at $x = L$ are

$$\hat{p}(L,y) = \lfloor \phi_m(y) \rfloor [\mathcal{Z}_m] \{\hat{u}_m^+\} \qquad (27)$$

$$\hat{u}(L,y) = \lfloor \phi_m(y) \rfloor \{\hat{u}_m^+\} \qquad (28)$$

Note that the modal impedance matrix $[\mathcal{Z}_m]$ is diagonal for the present case of an infinite duct. In the case of a finite duct, this matrix would contain the radiation impedances [4] of the duct termination and would *not* be diagonal. This are the only differences between the infinite and finite duct cases.

Now define the pressure and axial velocity at node points, or y-grid lines i, j, as

$$\hat{p}_i = \hat{p}(L,y_i) \qquad (29)$$

$$\hat{u}_j = \hat{u}(L,y_j) \qquad (30)$$

The pressure and axial velocity at each node point are then given in terms of the modal amplitude coefficients for the progressive waves in an infinite duct.

$$\{\hat{p}_i\} = [\phi_{im}][\mathcal{Z}_m]\{\hat{u}_m^+\} \tag{31}$$

$$\{\hat{u}_j\} = [\phi_{jm}]\{\hat{u}_m^+\} \tag{32}$$

$$\phi_{im} = \phi_m(y_i) \tag{33}$$

Eliminating the modal amplitudes gives an operator relation between the nodal values of pressure and axial velocity.

$$\{\hat{p}_i\} = [Z_{ij}]\{\hat{u}_j\} \tag{34}$$

where the *nodal* impedance matrix is defined as

$$[Z_{ij}] = [\phi_{im}][\mathcal{Z}_m][\phi_{jm}]^{-1} \tag{35}$$

Equation (35) defines the nodal impedance matrix used to construct the non-local boundary condition. This boundary condition insures continuity of the solutions at the interface between the interior and the exterior domains. Furthermore, the boundary condition, although constant, insures continuity for all possible exterior solutions. In other words, it represents the general solution in the exterior domain.

4 Numerical Results

In this section we validate the accuracy of the non-local boundary condition. The precise construction is given in appendix A. Exact attenuations were computed from the exact series solution for outgoing waves developed in appendix B. The exact series expression used 51 modes in the series solution. Sample calculations are presented for both rigid and soft wall ducts and for several sound sources. Each source oscillates at 100, 500, 1,000 and 5,000 Hertz. It is shown that the new condition can be applied very close to the source, rendering the computational domain small. All results were computed using a duct one meter in height with ambient values of $\bar{p}, \bar{\rho}$ and $\bar{c}$. The computation uses a grid aspect ratio of unity ($\Delta x = \Delta y$) for each calculation, with fifty-one evenly spaced points in the transverse direction. This grid was chosen because it allows approximately seven points per wavelength at the highest frequency of 5,000 Hertz. Although the calculations presented here will be of limited scope and represent only a small fraction of the total capability of the model, they do test the integrity of boundary condition formulation. The convergence characteristics and overall accuracy of the numerical model are also accessed.

Each figure is presented in the form of the schematic of figure (2). The vertical dotted lines indicate the location of the right boundary where the nonlocal boundary condition is applied. The vertical scale is a measure of the attenuation from the axial $x/H = 0$ to points $x/H = .1L/H, x/H = .2L/H, ..., x/H = 1.0L/H$ consecutively.

4.1 Results For A Rigid Wall Duct

The first set of calculations is for a rigid wall duct ($\beta = 0 + 0i$). These choices for the wall admittance are not due to a limitation of the method, but allow comparison with exact analytical results available for planar and point sources. No attenuation is possible for a planar or point source propagating down a hard wall duct. Figure (3) compares the exact value of attenuation to that computed using the current model for a planar source. Numerical results were computed by applying the new boundary condition closer and closer
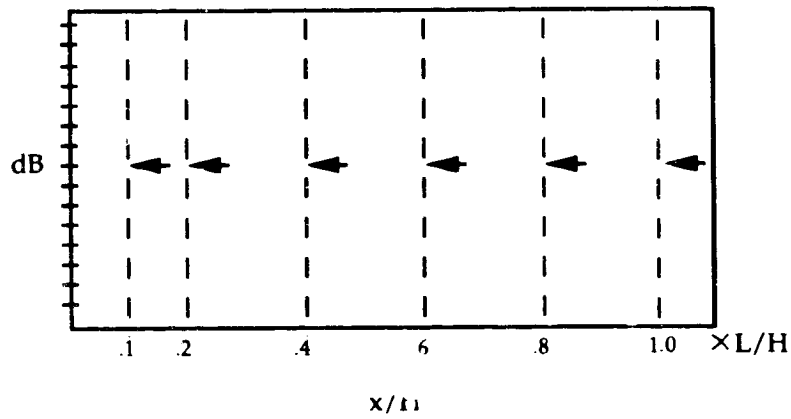
Figure 2: Axial locations where the nonreflecting boundary condition is applied, i.e. the six dotted vertical lines for $x > 0$ (at $x/H = .1, x/H = .2$ etc.) are the points of application of the boundary condition.
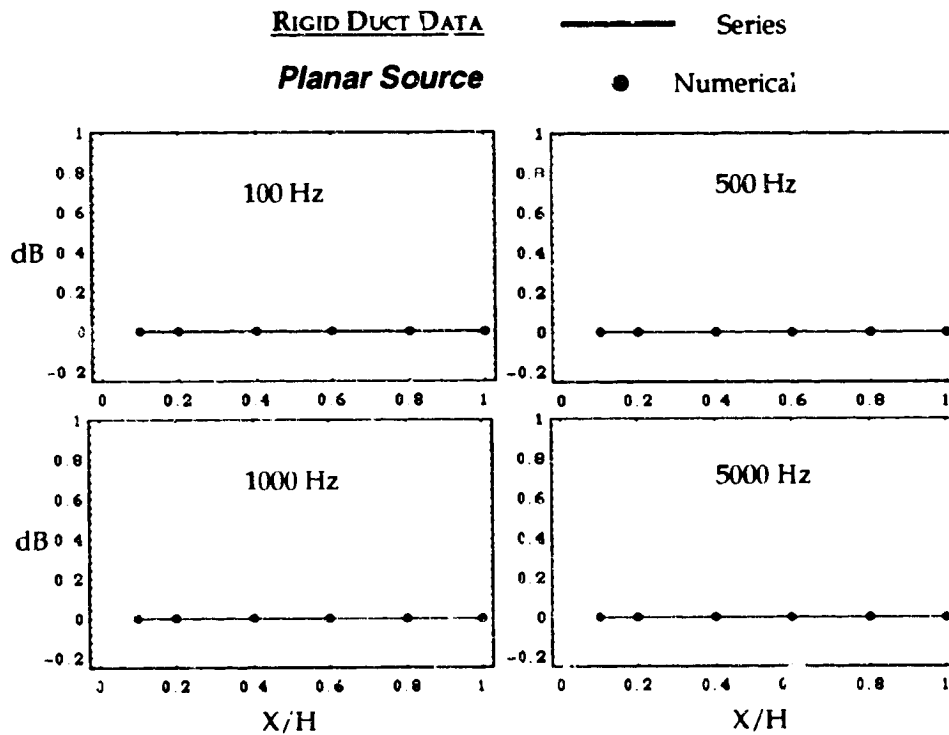

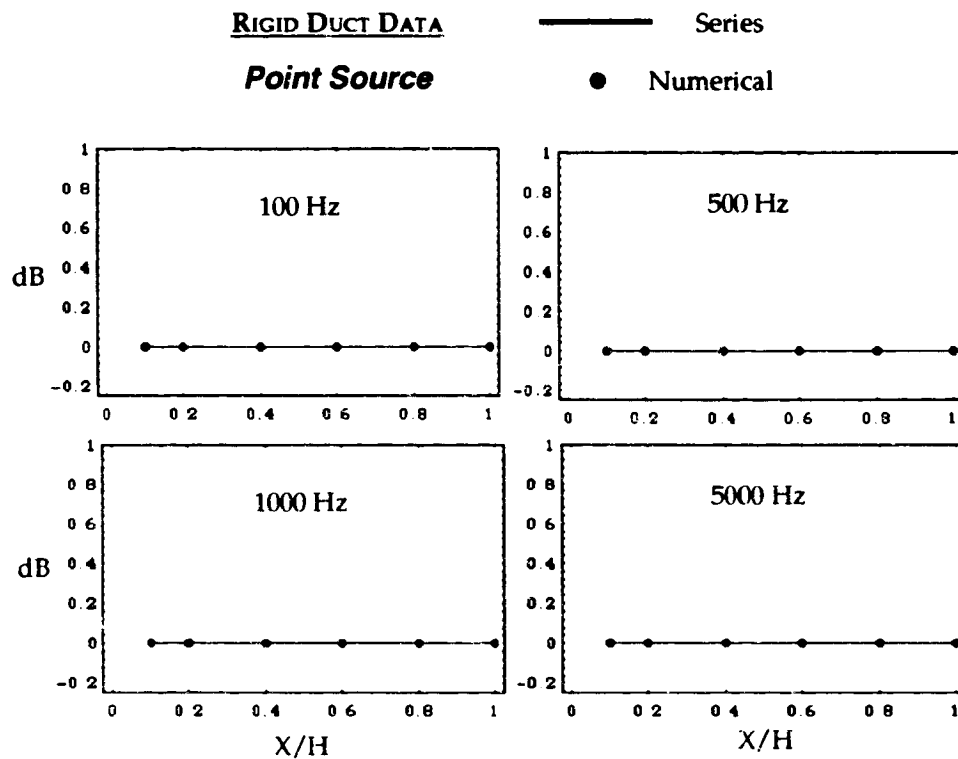Figure 3: Attenuation prediction for a planar source propagating in a hard wall duct.

11

Figure 4: Attenuation prediction for a point source propagating in a hard wall duct.

to the sound source and computing attenuation over that length for each of the frequencies. The boundary condition was applied at the following values of duct aspect ratio (L/H=1, L/H=.8, L/H=.6, L/H=.4, L/H=.2 and L/H=.1). Numerical predictions compare well to the exact value. There is no attenuation in either case.

Attenuation predictions for a point source in a hard wall duct located at $y = 0$ are compared to the exact series expression in figure (4). The point source attenuation comparisons are good for all frequencies and aspect ratios. Such good agreement for the point source is encouraging since a large number of planar modes are required for it full representation. Thus for rigid wall ducts, the boundary condition is accurate for a wide range of sources and may be applied close to the source.
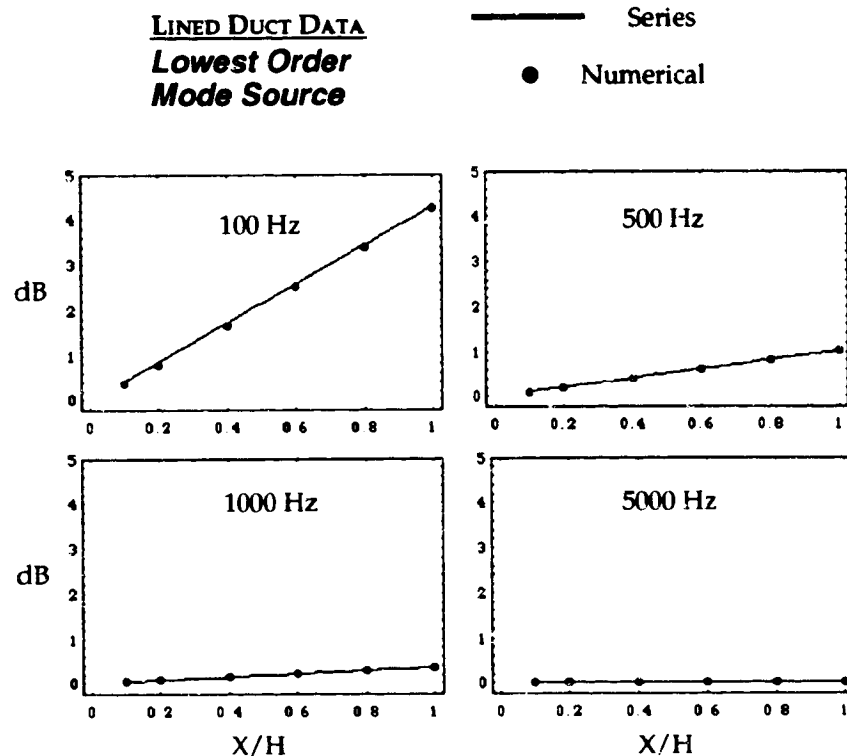
Figure 5: Attenuation prediction for a lowest order mode source propagating in a lined duct

4.2 Results With Wall Lining.

A major goal of computational methods is to guide the design of liners which will reduce broadband noise in the current generation of aircraft. Any useful computational boundary condition, must remain valid in the presence of a wall lining. Attenuation comparisons are shown in figure (5) where the sound source is the lowest order mode. The admittance of each wall was chosen as $\beta = .5 - .5i$. Good comparison between the finite element and modal theory has been obtained in the presence of the wall lining. Note also that the presence of the liner causes attenuation of the sound as it propagates down the duct.

Similar comparisons were obtained for a point source located at $y = 0$ with the same liner values. Results for the point source are plotted in figure (6). Again, attenuation predictions using the non-local boundary condition are generally in good agreement with results from the exact series solution. The exception is the 5000 Hz case where the computational solution does not have monotone variation of the attenuation. Monotone variation is an absolute
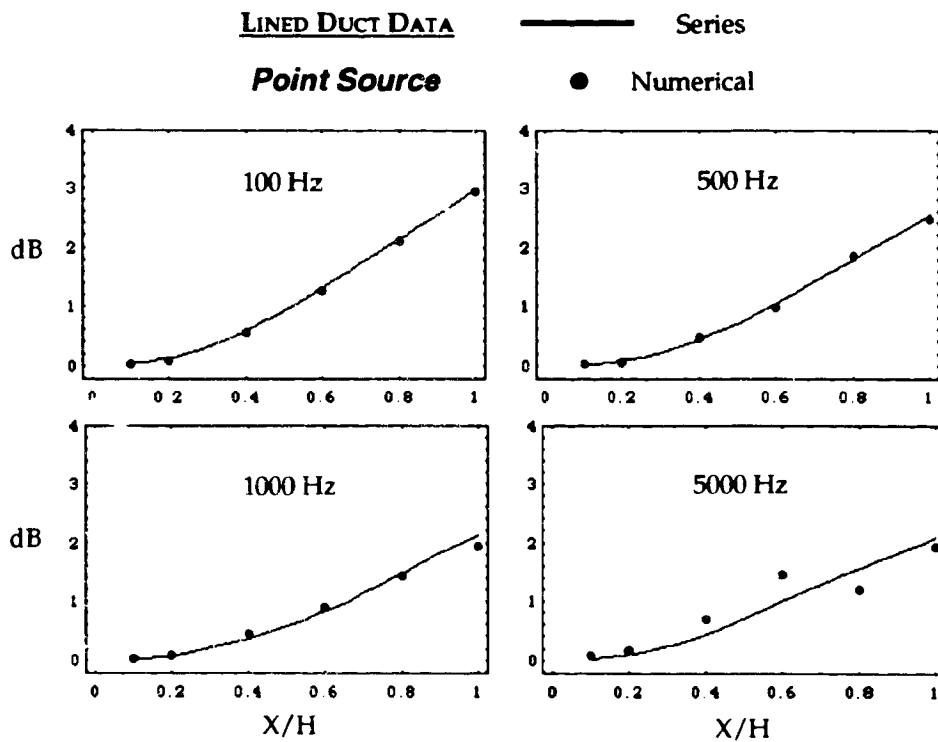
13

Figure 6: Attenuation prediction for a point source propagating in a lined duct.

requirement, since energy must be dissipated by the liner. It is possible that the error observed here is due to the small number of points/wavelength in this high frequency case. Further study will be needed to resolve this question.

5 Concluding Remarks

A non-local boundary condition has been developed for numerically simulating acoustic waves in ducts without flow. The non-local boundary condition represents the general solution to a linear wave equation in an unbounded exterior domain. The case of an infinite duct was used here for simplicity, but the boundary condition can represent the general solution for radiation from finite ducts as well.

The boundary condition was applied to the case of two-dimensional, constant area ducts with constant impedance wall linings. Extension of the method to three-dimensional ducts is straightforward in principle, but requires significantly more computation. The boundary condition can be applied without change to variable-area ducts as long as the exterior domain represented by the boundary condition has constant area. Similarly, it can be applied to variable-impedance duct sections coupled to a constant-impedance duct termination. The boundary condition will represent finite ducts if the diagonal modal impedance matrix is replaced by a non-diagonal radiation impedance matrix.

A finite element solution is developed which utilizes the boundary condition to limit the computational space while preserving the radiation boundary condition. The solution algorithm allows calculations for large numbers of computational points and high frequencies.

The effectiveness of the new boundary condition has been evaluated by comparing predicted sound attenuations with exact analytical results available from modal theory. The boundary condition was tested for both single mode and point sources at several frequencies using 3.4 or more points per axial wavelength. Excellent comparisons with exact analytical results were obtained with and without wall linings for most cases considered. The single exception was the highest frequency case in a lined duct which had only the minimum of 3.4 points per wavelength. In this case, a small negative attenuation was observed in a part of the computational solution.

It has been demonstrated that the boundary condition gives accurate results when the point of application is brought close to the sound source. This is an important result in

computational aero-acoustics, since conserving grid points is a major concern.

The boundary condition should be extended to the case of acoustic waves in the presence of steady flow. This extension will require the consideration of vortical and entropic modes which have been ignored here. The extension appears possible, however, since the only real requirement of the method is that the aeroacoustic field in the exterior domain is given by the general solution of a set of linear equations.

References

[1] Zorumski, W. E.: Classical Theoretical Approaches to Computational Aeroacoustics, pp 41–49 in *Computational Aeroacoustics*, J. C. Hardin and M. Y. Hussaini, Editors. Springer-Verlag Inc., New York, 1993.

[2] Enquist, B.; and Majda, A. : Absorbing Boundary Conditions for the Numerical Simulation of Waves. *Journal of Computational Physics*, Vol. 31 No. 139, 1977

[3] Pierce, A.D.: Acoustics: An Introduction to Its Physical Principles and Applications. Acoustical Society of America, 1989.

[4] Zorumski, William E.: Generalized Radiation Impedance and Reflection Coefficients of Circular and Annular Ducts. *Journal of the Acoustical Society of America*, Vol. 54, No. 6, December 1973.

[5] Zienkiewicz, O.C.: The Finite Element Method In Engineering Science, McGraw-Hill Book Company, London, 1971.

[6] Desai, Chandrakant S.; and Abel, John F.: Introduction To The Finite Element Method, Van Nostrand Reinhold Company, New York,N.Y. 1972.

[7] Eversman, W.: Energy Flow Criteria for Acoustic Propagation in Ducts with Flow, *Journal of the Acoustical Society of America*, Vol. 49, No. 6, June 1971.

[8] Abrahamson, A.L.: A Finite Element Algorithm for Sound Propagation in Axisymmetric Ducts Containing Compressible Mean Flow. NASA CR-145209 , June 1977.

A   The Numerical Method

The numerical method chosen to solve equation 8 coupled with the source, nonreflecting, and wall boundary conditions is a Galerkin finite-element method. Details on the method for structural vibrations problems are given in several texts [6, 5] and only sufficient detail is presented here to highlight important differences for the current duct acoustics problem. When applied to the current problem, the finite-element method may be interpreted as a physical visualization of the continuous pressure field as an assemblage of rectangular elements interconnected at nodes as illustrated in figure 7. It is assumed that there are N nodes in the axial and M nodes in the transverse direction of the duct as illustrated in the upper half of the figure. A typical rectangular element, $[I, J]$ is shown in the lower half of the figure. Each element consists of four nodes labeled 1,2,3 and 4,respectively. A typical element is considered to have width a and height b as shown. The objective of the method is to obtain the unknown acoustic pressure at the nodes of each of the $(M-1)(N-1)$ elements.

Galerkin's finite element method is employed to minimize the error vector. This reduces the problem to a finite set of algebraic equations which are solved using matrix methods. Define the error function as:

$$E(x,y) = \nabla^2 \hat{p} + k^2 \hat{p} + S \tag{36}$$

Within each element $\hat{p}$ and S are represented as linear functions:

$$\hat{p}(x,y) = \sum_{I=1}^{I=4} N_I(x,y)\hat{p}_I, \quad S(x,y) = \sum_{I=1}^{I=4} N_I(x,y)S_I \tag{37}$$

$$N_1(x,y) = (1 - \frac{x}{\Delta x})(1 - \frac{y}{\Delta y}), \quad N_2(x,y) = \frac{x}{\Delta x}(1 - \frac{y}{\Delta y}) \tag{38}$$

$$N_3(x,y) = \frac{x}{\Delta x}\frac{y}{\Delta y}, \quad N_4(x,y) = (1 - \frac{x}{\Delta x})\frac{y}{\Delta y} \tag{39}$$

in which $\hat{p}_I, S_I$, are the values of $\hat{p}$ and S respectively at node I. The variable admittance β is represented in a similar manner along each boundary element. The correct solution to the sound field is obtained when the error $E(x,y)$ is identically zero at each point of the domain. This is approximately achieved by requiring that the error function be orthogonal
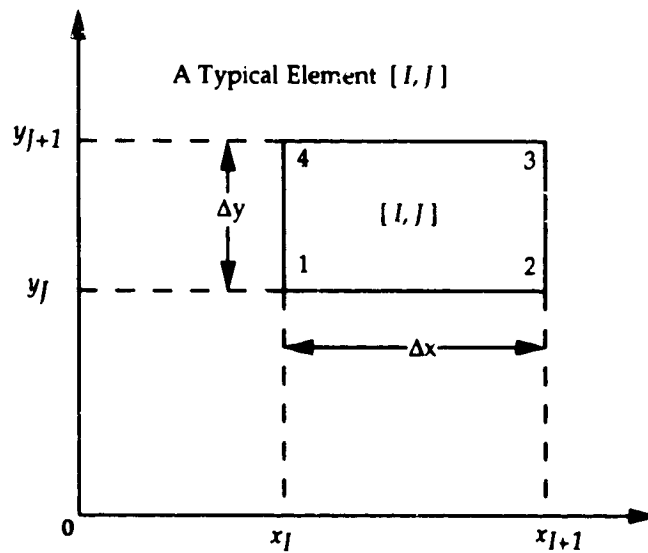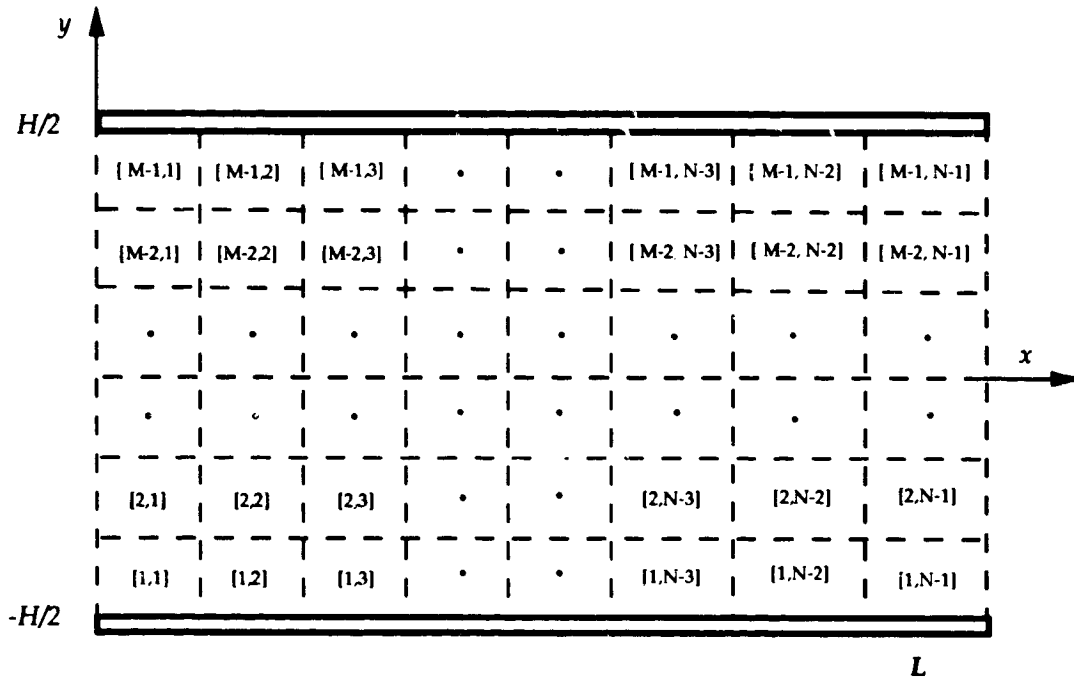
18

Figure 7: Finite element discretization and numbering system for the computational domain.

to each basis function $N_I(x, y)$ that are assumed to represent a complete set of functions. Contributions to the minimization of the error function from a typical element is

$$\int_0^a \int_0^b E(x, y) N_I(x, y) dy dx = [A_{ij}^e]\{\Phi_j^e\} + \{F_j^e\} \qquad (40)$$

Where $[A_{ij}^e]$ is a 4x4 complex matrix (i.e. the stiffness matrix) $\{\Phi_j^e\}$ is a 4x1 column vector containing the unknown acoustic pressure at the four nodes of the element, and $\{F_j^e\}$ is a 4x1 column vector containing source effects. The coefficients in the local stiffness matrix $[A_{ij}^e]$ were computed in closed form and are not written explicitly in this work. The second derivative terms in equation (40) were integrated by parts in order that linear basis functions could be used and the effects of the wall boundary conditions included.

Assembly of the global equations for the computational domain is a basic procedure in the finite element method. Appropriate shifting of rows and columns is all that is required to add the local element matrix $[A_{ij}^e]$ directly into the global matrix $[A_{ij}]$. A similar method is used to construct $\{F_j\}$ from $\{F_j^e\}$. Assembling the elements for the entire domain results in a matrix equation of the form:

$$[A_{ij}]\{\Phi_j\} = \{F_j\} \qquad (41)$$

where $[A]$ is an $MN \times MN$ complex matrix, and $\{\Phi_j\}$ is a $MN \times 1$ column vector containing the values of the unknown acoustic pressures at the MN nodes of the duct. It is necessary to apply the source pressure, and termination condition to this system of equations before a unique solution can be obtained. Satisfying the noise source boundary condition consists simply of setting all nodal values of acoustic pressure at the source plane ($x = 0$) to the known value of source pressure. Provisions are made for insertion of this conditions into the assembled global matrix equation equation (41). Further details on this method of imposing source conditions are described elsewhere [8, 5, 6] and are not repeated here.

The nonreflecting condition given by equation (11) must be imposed on the matrix equation before the solution can be obtained. The axial velocity vector, $\{\hat{u}\}$ may be expressed

20

as a single equation on the acoustic pressure from the second of equation (3)

$$\{\hat{u}_i\} = \frac{i}{\omega\bar{\rho}}\frac{\partial}{\partial x}\{\hat{p}_i\} \tag{42}$$

Substituting equation (42) into equation (11) gives a system of constraint equations relating the acoustic pressures along the nodes at $x = L$ ($\{\hat{p}_i\}$) and those one grid point to the left of $x = L$ ($\{\hat{p}_{jL}\}$)

$$[\overline{Z_{ij}}]\{\hat{p}_j\} = \frac{[Z_{ij}]}{i\omega\bar{\rho}(x_N - x_{N-1})}\{\hat{p}_{jL}\} \tag{43}$$

$$[\overline{Z_{ij}}] = \left[\frac{1}{i\omega\bar{\rho}(x_N - x_{N-1})}[Z_{ij}] + [I]\right] \tag{44}$$

where $[I]$ is the identity matrix. Equations(43) are a set of constraint equations ensuring outgoing acoustic waves in the second section of duct. Standard finite element techniques are used to incorporate (43) into equation (41) using the Lagrange multiplier technique [5].

The global matrix $[A_{ij}]$ generated by Galerkin's Method following application of the source and constraint equations is a positive indefinite, complex matrix. Fortunately, owing to the discretization scheme used it will be block tridiagonal. The structure of matrix $[A_{ij}]$ is shown in figure 8. Note that it is a square block tridiagonal matrix whose order is MN. This global matrix contains a number of major blocks ($[A_I], [B_I]$ and $[D_I]$) which are themselves square and tridiagonal with the structure shown in figure 9. Note that each minor block $[A_I], [B_I]$ and $[D_I]$ is a square tridiagonal matrix whose order is M. Much practical importance arises from this structure as it is convenient for minimizing storage and maximizing computational efficiency. Economy of storage is acheived by storing the rectangular array of coefficients within the bandwidth of $[A_{ij}]$ as shown in figure 10

All computation,storage and boundary condition implementation is performed on this rectangular structure. Special matrix techniques exist for a solution of this structure. Gaussian elimination with partial pivoting and equivalent row infinity norm scaling is used to obtain the solution to this rectangular system. All computations were performed on Langley's Cray-2S ccmputer.
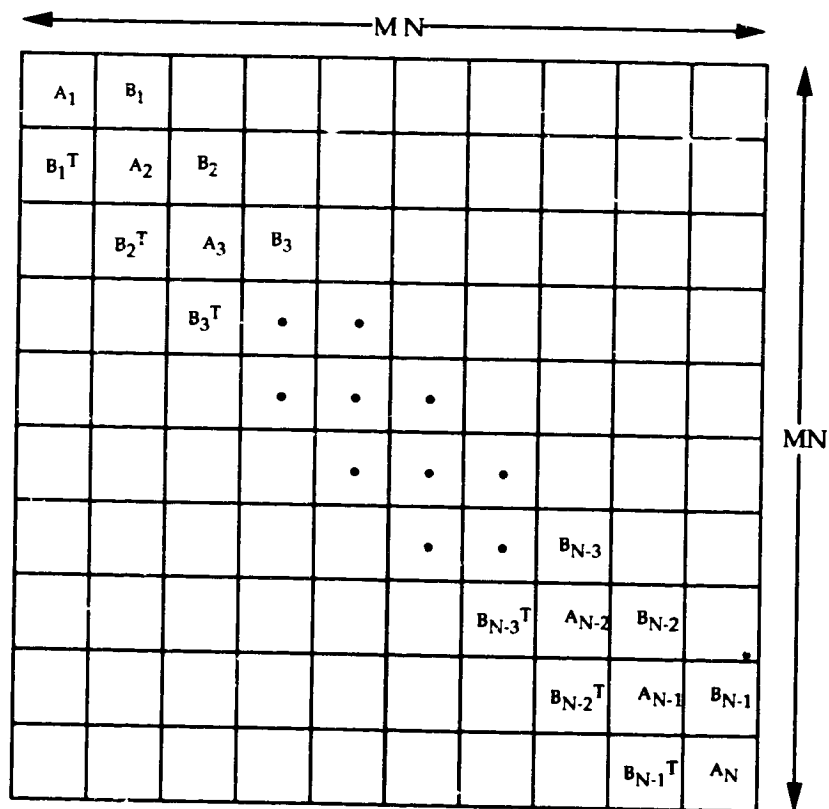
21

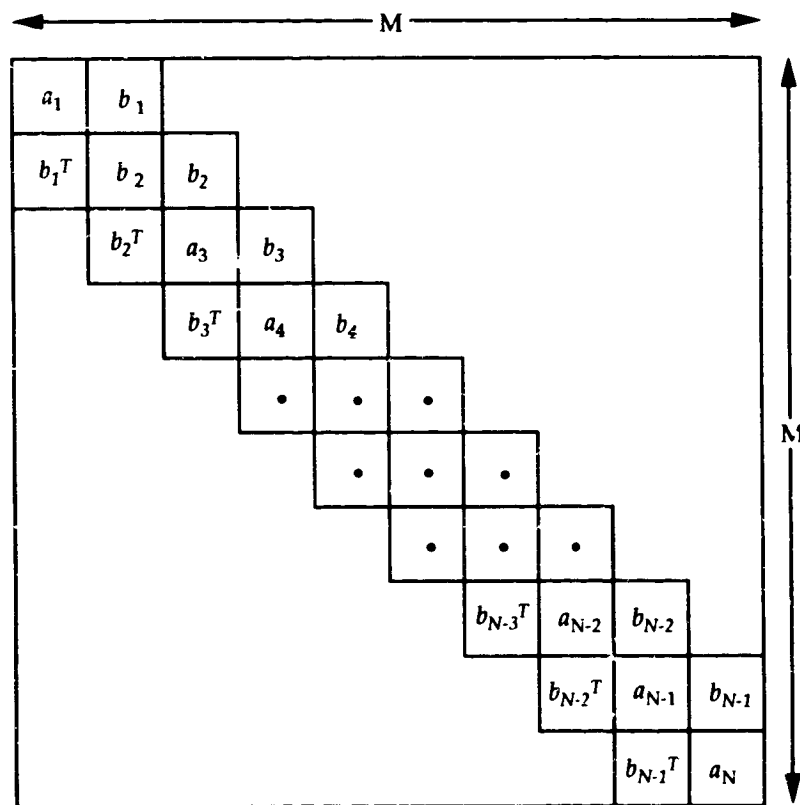Figure 8: Structure of the global stiffness matrix, A with minor blocks.

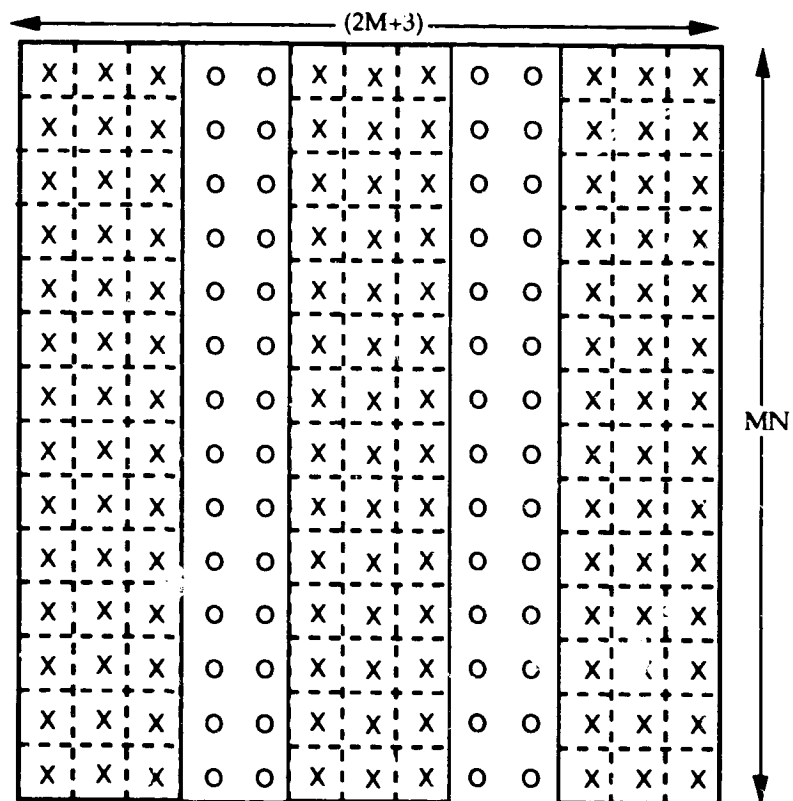Figure 9: Structure of each minor block A_I and B_I.

Figure 10: The stored $MN \times (2M+3)$ rectangular coefficient matrix with nonzero coefficients X.

B Eigenvalue Computation

B.1 High Order Eigenvalues

When the walls are hard, the eigenvalues are multiples of π, but when the walls have finite admittances, a complex characteristic equation must be solved for the eigenvalues. This can easily be the most difficult part of the computation, so the method is developed here in considerable detail. We group the admittance at the wall with the frequency parameter kH by defining $\tau_0 \equiv \bar{\rho}\bar{c}\beta_0 kH$ and $\tau_H \equiv \bar{\rho}\bar{c}\beta_2$.

The eigenvalue computation procedures shown here were written independently of the rest of the paper and, purely by chance, used the time factor $\exp\{-i\omega t\}$. All complex variables with this convention are the complex conjugates of the variables in the body of this paper so that the eigenvalue equation 19 must be conjugated, giving the following eigenvalue equation.

$$1 - e^{2ik_yH}\left(\frac{1 - \frac{\tau_H}{k_yH}}{1 + \frac{\tau_H}{k_yH}}\right)\left(\frac{1 - \frac{\tau_0}{k_yH}}{1 + \frac{\tau_0}{k_yH}}\right) = 0 \tag{45}$$

In the case of hard walls, where $\tau_0 = \tau_H = 0$, solutions to equation 45 are

$$k_yH = m\pi, \quad m = 0, 1, 2, \cdots \tag{46}$$

This elementary case suggests the definition

$$(k_yH)_m = m\pi + \delta_m, \quad m = 0, 1, 2, \cdots \tag{47}$$

B.1.1 Characteristic equation for higher modes, $m > 0$

The characteristic equation for the higher modes can be given in logarithmic form as

$$F(\delta_m) = 0 \tag{48}$$

$$F(\delta_m) = \delta_m + \frac{i}{2}\log\left[1 + \frac{\tau_0}{m\pi + \delta_m}\right] + \frac{i}{2}\log\left[1 + \frac{\tau_H}{m\pi + \delta_m}\right]$$
$$- \frac{i}{2}\log\left[1 - \frac{\tau_0}{m\pi + \delta_m}\right] - \frac{i}{2}\log\left[1 - \frac{\tau_H}{m\pi + \delta_m}\right] \tag{49}$$

It is clear from this form of the characteristic equation that the solution δ_m approaches zero in the limit where $m \to \infty$. The points where $m\pi + \delta_m = \pm\tau_{0,H}$ are singularities of F which

cannot be solutions. These points should not cause difficulty except possibly in the case where $m = 0$. The explicit form of equation 49 is important. Computing each logarithim separately avoids crossing the branch cut, which could introduce an error of π in the value of the complex log.

B.1.2 Newtons method solution for higher modes

Newtons method numerical solutions of equation 48 utilize an iteration for δ_m given by the replacement operation

$$\delta_m \leftarrow \delta_m - \frac{F(\delta_m)}{F'(\delta_m)} \tag{50}$$

where the derivative of the characteristic function is

$$F'(\delta_m) = 1 - i\frac{\tau_0}{(m\pi + \delta_m)^2 - \tau_0^2} - i\frac{\tau_H}{(m\pi + \delta_m)^2 - \tau_H^2} \tag{51}$$

This solution method is very effective for higher modes $m > 1$. One can quickly generate a thousand or more eigenvalues on a modern workstation. The work in developing a useful basis for a modal computation is then limited to computing the lower eigenvalues. This computation is discussed below.

B.2 Low Order Eigenvalues

B.2.1 Alternate form of the characteristic equation

The Newtons method is fast and dependable for the case where $m > 1$, but special care is needed for the cases where $m = 0$ or $m = 1$. The problem is worst when the admittances have large imaginary parts and small real parts, so we attack these cases first. In these cases, there may be pure imaginary solutions for the eigenvalue $K_y H$. Accordingly the following definitions are introduced to investigate these cases.

$$K_y H = -i\eta \tag{52}$$

$$a = -\tau_0 \tau_H \tag{53}$$

$$b = -i\frac{\tau_0 + \tau_H}{2} \tag{54}$$

26

These changes of variable allow the characteristic equation to be expressed as

$$F(\eta) = a + \eta^2 + 2i\eta \coth \eta = 0 \tag{55}$$

To this point, there has been no real change, since all variables are complex. Now consider solutions where the parameters a, b are real variables, that is, the real parts of the complex parameters defined above. We can find real solutions ξ for these real parameters and add the effects of their imaginary parts later

B.2.2 Solutions for real parameters

Now take the real parts a_1, b_1 of the parameters $a = a_1 + ia_2$, $b = b_1 + ib_2$, but, for brevity, use the same symbols a, b with the understanding that they are restricted to real values in this subsection. When the parameters are real, a better form of the characteristic equation utilizes the square of the eigenvalue.

$$\xi = \eta^2 = -(K_y H)^2 \tag{56}$$

$$F(\xi) = a + \xi + 2b\frac{C(\xi)}{S(\xi)} \tag{57}$$

$$C(\xi) \equiv \cosh \eta \tag{58}$$

$$S(\xi) \equiv \frac{\sinh(\eta)}{\eta} \tag{59}$$

The value of the characteristic function at the origin and its behavior when ξ is large are important for the determining if the characteristic function has zeros for positive ξ.

$$F(0) = a + 2b \tag{60}$$

$$F(\xi) \sim \xi, \quad \xi \to \infty \tag{61}$$

The defined functions $C(\xi)$ and $S(\xi)$ have properties which make them useful in determining solutions to the characteristic equation. These properties will be listed here before considering the numerical proceedure for solving for the eigenvalues.

The functions are defined by the series for the hyperbolic functions.

$$C(\xi) = \sum_{n=0}^{\infty} \frac{\xi^n}{(2n)!} \tag{62}$$

$$S(\xi) = \sum_{n=0}^{\infty} \frac{\xi^n}{(2n+1)!} \tag{63}$$

The series definitions permit the following immediate observations.

$$S(\xi) \leq C(\xi), \quad 0 \leq \xi < \infty \tag{64}$$

$$S'(\xi) \leq C'(\xi), \quad 0 < \xi < \infty \tag{65}$$

$$1 \leq C(\xi), \quad 0 \leq \xi < \infty \tag{66}$$

$$\frac{1}{2} \leq C'(\xi), \quad 0 \leq \xi < \infty \tag{67}$$

$$1 \leq S(\xi), \quad 0 \leq \xi < \infty \tag{68}$$

$$\frac{1}{6} \leq S'(\xi), \quad 0 \leq \xi < \infty \tag{69}$$

The following formulas are useful for evaluating the derivatives of the functions.

$$C'(\xi) = \frac{1}{2}S(\xi) \tag{70}$$

$$S'(\xi) = \frac{C(\xi) - S(\xi)}{2\xi} \tag{71}$$

Finally, the functions have the following asymptotic character.

$$S(\xi) \sim \xi^{-1/2}C(\xi), \quad \xi \to \infty \tag{72}$$

$$S'(\xi) \sim \frac{1}{2}\xi^{-1}C(\xi), \quad \xi \to \infty \tag{73}$$

$$C'(\xi) \sim \frac{1}{2}\xi^{-1/2}C(\xi), \quad \xi \to \infty \tag{74}$$

The first derivative of the characteristic function is

$$F'(\xi) = 1 + \frac{b}{S^2(\xi)}\left(\frac{C(\xi)S(\xi) - 1}{\xi}\right) \tag{75}$$

$$F'(0) = 1 + \frac{2}{3}b \tag{76}$$

$$F'(\xi) \sim 1 + b\xi^{-1/2}, \quad \xi \to \infty \tag{77}$$

28

The derivative $F'(\xi)$ approaches unity from above or below, depending on the sign of b, wnen ξ is large. The derivative $F'(0)$ may be positive or negative, depending on the value of b. It is positive for $b > -3/2$, zero for $b = -3/2$, and negative for $b < -3/2$. The second derivative of the characteristic function is

$$F''(\xi) = -\frac{b}{S^3(\xi)}\left[\frac{C(\xi)(S^2(\xi) - 2) + S(\xi)}{2\xi^2}\right] \tag{78}$$

$$F''(0) = -\frac{4}{45}b \tag{79}$$

$$F''(\xi) \sim -\frac{b}{2}\xi^{-3/2}, \quad \xi \to \infty \tag{80}$$

The function within brackets is positive, so that the sign of the   ond derivative depends only on the sign of b. If b is negative the curvature is positive, and if b is positive, the curvature is negative. The limit of the function within brackets is $4/45$ for $\xi = 0$, giving the value of the derivative at the origin.

Small solutions $|\xi| << 1$ are possible for certain combinations of the paramaters a, b. These combinations are identified by utilizing a two-term series for the characteristic function.

$$F(\xi) = F(0) + F'(0)\xi = 0 \tag{81}$$

which gives the following estimate for η^2

$$\xi = -\left(\frac{a + 2b}{1 + \frac{2}{3}b}\right) \tag{82}$$

In order for this estimate to be consistent with the assemed smallness of ξ, the parameters must be related by

$$-|F'(0)|\,\epsilon \leq F(0) \leq +|F'(0)|\,\epsilon \tag{83}$$

$$-\left|1 + \frac{2}{3}b\right|\epsilon \leq F(0) \leq +\left|1 + \frac{2}{3}b\right|\epsilon \tag{84}$$

In the special case where $\dot{v} \to -3/2$, the limits above show that $a \to -2b$. These solutions may be positive or negative since they represent the effect of the parameters in moving the solutions from the real $K_y H$ axis to the imaginary $K_y H$ axis in the neighborhood of the origin.

There are a long list of cases to investigate in determining whether solutions for $K_y H$ exist near the origin or on the imaginary axis (ξ is positive). The cases will be organized here by defining ranges of the characteristic function and its slope at the origin. These parameters ($F(0)$ and $F'(0)$) depend on the parameters a, b only.

1. If $F'(0) > +\epsilon$, the slope of the characteristic function is positive everywhere and, if $F(0) > +\epsilon$, there is no positive solution, however

   (a) if $|F(0)| \leq \epsilon$, there is a small solution, $\xi = O(\epsilon)$, or

   (b) else if $F(0) < -\epsilon$, there is a positive solution $\xi > 0$ or

2. else if $|F'(0)| \leq \epsilon$, the slope at the origin is near zero and if $F(0) > +\epsilon^2$, there is no positive solution, however

   (a) if $|F(0)| \leq \epsilon^2$, there is a small double solution $\xi = O(\epsilon)$, or

   (b) else if $F(0) < -\epsilon^2$, there is a positive solution, or

3. else if $F'(0) < -\epsilon$, the slope at the origin is negative and the characteristic function has a minimum for some $\xi > 0$. Find the location of the minimum ξ_{min} and evaluate the characteristic function to get its minimum value F_{min}. If $F_{min} > \epsilon^2$, there is no solution, however

   (a) if $|F_{min}| \leq \epsilon^2$, there is a double solution near ξ_{min}, or

   (b) else if $F_{min} < -\epsilon^2$, the solutions depend on the value of F at the origin.

       i. If $F(0) > +\epsilon^2$, there are two distinct solutions $\xi < \xi_{min}$ and $\xi > \xi_{min}$, or

       ii. else if $|F(0)| \leq \epsilon^2$, there is a solution near $\xi = 0$ and another solution $\xi > \xi_{min}$, or

       iii. else if $F(0) < -\epsilon^2$, there is a single solution $\xi > \xi_{min}$.

B.2.3 Solutions for complex parameters

Having found all possible solutions for real parameters, the next step is to find the effect of the imaginary parts of the parameters on these solutions. Let the parameters a, b be complex functions of a real parameter s which varies from zero to unity, $0 \leq s \leq 1$. The parameters are identical to their real parts when $s = 0$ and take their actual values when $s = 1$. Begin with the solutions for real parts of the parameters in the case where $s = 0$ and trace these solutions to the point where $s = 1$. Note that these solutions can include effects of the real parts of the admittances in the parameter a. The tracing follows a differential equation for the square of the eigenvalue $\xi(s)$ as a function of the parameter s.

$$K_y(s)H = \sqrt{-\xi(s)} \tag{85}$$

$$a = -\tau_0 \tau_H \tag{86}$$

$$b = -i\frac{\tau_0 + \tau_H}{2} \tag{87}$$

$$a(s) = \Re[a] + i\Im[a]s = a_1 + ia_2 s \tag{88}$$

$$b(s) = \Re[b] + i\Im[b]s = b_1 + ib_2 s \tag{89}$$

Now, $\xi(s)$, $a(s)$, and $b(s)$ are complex functions of the real variable s. The characteristic function depends on s, and is complex, but is otherwise unchanged from the one defined for real variables.

$$F(\xi; s) = a(s) + \xi + 2b(s)\frac{C(\xi)}{S(\xi)} \tag{90}$$

$$\frac{\partial F(\xi; s)}{\partial \xi} = 1 + b(s)\left(\frac{C(\xi)S(\xi) - 1}{\xi S^2(\xi)}\right) \tag{91}$$

$$\frac{\partial^2 F(\xi; s)}{\partial \xi^2} = -\frac{b(s)}{S^3(\xi)}\left[\frac{C(\xi)(S^2(\xi) - 2) + S(\xi)}{2\xi^2}\right] \tag{92}$$

$$\frac{\partial F(\xi; s)}{\partial s} = a'(s) + 2b'(s)\frac{C(\xi)}{S(\xi)} \tag{93}$$

The solutions where $s = 0$ are initial conditions for a first-order differential equation which is used to find $\xi(s)$.

$$d\xi = -\frac{\left(\frac{\partial F}{\partial s}\right)}{\left(\frac{\partial F}{\partial \xi}\right)}ds \tag{94}$$

31

This equation is valid as long as the initial condition is not a double eigenvalue. When the initial condition is a double eigenvalue ξ_m, the partial derivative in the denominator is

$$\frac{\partial F}{\partial \xi} = \frac{\partial^2 F(\xi; s)}{\partial \xi^2}(\xi - \xi_m) \tag{95}$$

The differential equation for ξ is then singular, but a differential equation for the square of the displacements of the eigenvalues from the double eigenvalue is not.

$$d(\xi - \xi_m)^2 = -2\frac{\left(\frac{\partial F}{\partial s}\right)}{\left(\frac{\partial^2 F}{\partial \xi^2}\right)} ds \tag{96}$$

Given an initial step Δs, the two eigenvalues near the double eigenvalue are

$$\xi = \xi_m \pm \sqrt{-2\frac{\left(\frac{\partial F}{\partial s}\right)}{\left(\frac{\partial^2 F}{\partial \xi^2}\right)}\Delta s} \tag{97}$$

The differential equation for the eigenvalue is then used to trace each of these to the final value for $s = 1$.

REPORT DOCUMENTATION PAGE

Public reporting burden for this collection of information is estimated to average 1 hour per response, including the time for reviewing instructions, searching existing data sources, gathering and maintaining the data needed, and completing and reviewing the collection of information. Send comments regarding this burden estimate or any other aspect of this collection of information, including suggestions for reducing this burden to Washington Headquarters Services, Directorate for Information Operations and Reports, 1215 Jefferson Davis Highway, Suite 1204, Arlington, VA 22202-4302, and to the Office of Management and Budget, Paperwork Reduction Project (0704-0188), Washington, DC 20503

1. AGENCY USE ONLY (Leave blank)	2. REPORT DATE March 1994	3. REPORT TYPE AND DATES COVERED Technical Memorandum

4. TITLE AND SUBTITLE A Non-local Computational Boundary Condition for Duct Acoustics	5. FUNDING NUMBERS 505-59-52
6. AUTHOR(S) William. E. Zorumski Willie R. Watson Steve L. Hodge	

7. PERFORMING ORGANIZATION NAME(S) AND ADDRESS(ES) NASA Langley Research Center Hampton, VA 23681-0001	8. PERFORMING ORGANIZATION REPORT NUMBER

9. SPONSORING/MONITORING AGENCY NAME(S) AND ADDRESS(ES) National Aeronautics and Space Administration Washington, DC 20546-0001	10. SPONSORING/MONITORING AGENCY REPORT NUMBER NASA TM-109091

11. SUPPLEMENTARY NOTES

12a. DISTRIBUTION AVAILABILITY STATEMENT Unclassified-Unlimited Subject Category 71	12b. DISTRIBUTION CODE

13. ABSTRACT (Maximum 200 words)

A non-local boundary condition is formulated for acoustic waves in ducts without flow. The ducts are two-dimensional with constant area, but with variable impedance wall lining. Extension of the formulation to three-dimensional and variable area ducts is straightforward in principle, but requires significantly more computation. The boundary condition simulates a non-reflecting wavefield in an infinite duct. It is implemented by a constant matrix operator which is applied at the boundary of the computational domain. An efficient computational solution scheme is developed which allows calculations for high frequencies and long duct lengths. This computational solution utilizes the boundary condition to limit the computational space while preserving the radiation boundary condition. The boundary condition is tested for several sources. It is demonstrated that the boundary condition can be applied close to the sound sources, rendering the computational domain small. Computational solutions with the new non-local boundary condition are shown to be consistent with the known solutions for nonreflecting wavefields in an infinite uniform duct.

14. SUBJECT TERMS Computational Methods, Computational Boundary Conditions, Computational Aeroacoustics	15. NUMBER OF PAGES 34
	16. PRICE CODE A03

17. SECURITY CLASSIFICATION OF REPORT Unclassified	18. SECURITY CLASSIFICATION OF THIS PAGE Unclassified	19. SECURITY CLASSIFICATION OF ABSTRACT Unclassified	20. LIMITATION OF ABSTRACT

NSN 7540-01-280-5500